

# MOCVD Growth Calibration for GaN LED on Silicon

Yusi Chen and Jieyang Jia

SNF Mentor: Dr. Xiaoqing Xu

Faculty advisor: Prof. James S. Harris

June 5<sup>th</sup>, 2015

## **Abstract**

Group-III-nitride materials have received significant research interest in the past decades due to the application of high-brightness UV/blue/white light LED. Our work is to calibrate the MOCVD growth of high quality group-III-nitride (III-N) materials on Si substrate for LED applications. We focuses our efforts on investigating the growth and annealing conditions to control the doping density in GaN and AlGaN and the composition in InGaN. We successfully demonstrated n- and p-type GaN grown in the MOCVD system in SNF and high-quality InGaN with indium percentage as high as 45%. Our work provides valuable information to future SNF users who will grow III-N materials for any optoelectronic application.

## **I. Motivation**

III-N materials grown by metal-organic-chemical-vapor-deposition (MOCVD) have attracted great research attention recently, especially with the three scientists winning Nobel Prize in Physics in 2014 “for the invention of efficient blue light-emitting diodes, which has enabled bright and energy-saving white light sources” [1]. The III-N based light-emitting-diode (LED) technology has disrupted the lighting industry that had been stable over 100 years. Right now 53.8% of the street lighting is provided by LEDs, and the number is projected to be increased to 93.8% by 2023 [2].

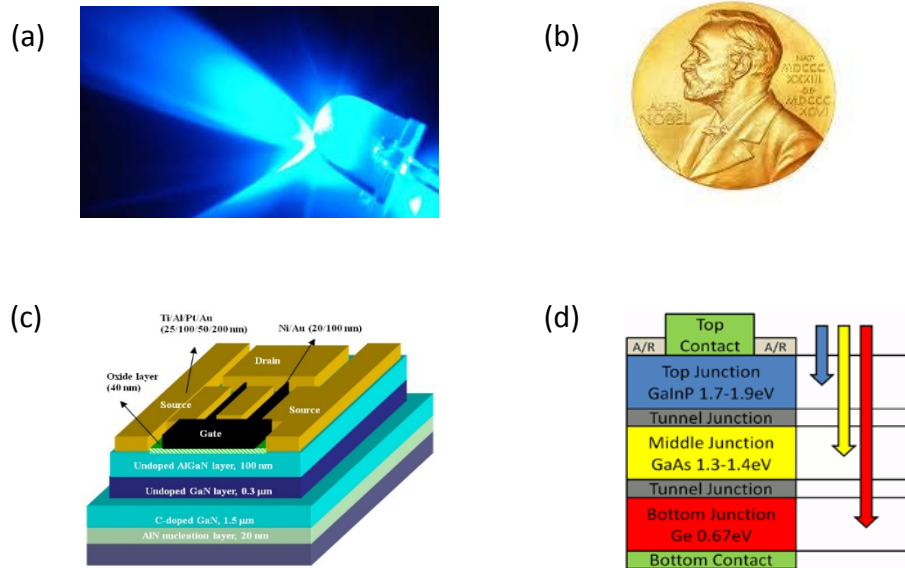


Figure 1. Applications of III-N MOCVD growth. (a) Blue LED [2]. (b) Nobel Prize in Physics, 2014 [1]. (c) High-Electron-Mobility-Transistor (HEMT) [3]. (d) High-efficiency multi-junction solar cells [4].

However, due to the lack of suitable homo-substrates, commercially LEDs available are mostly grown on costly sapphire or SiC substrates. On the other hand, Si substrates are widely used in semiconductor industry, and the usage of Si substrates offers many advantages, including low cost and high fabrication flexibility. Nevertheless, in order to grow III-N on Si, a variety of problems need to be solved and many researchers have put considerable effort into this field [3-8].

Recently SNF has introduced a new Axitron-CCS III-N MOCVD system (<https://snf.stanford.edu/SNF/equipment/chemical-vapor-deposition/mocvd/aix-ccs>) and it offers a variety of new opportunities for researchers and industry members of SNF who might be interested in III-N technology. However, since the system is new, not a lot of recipes are available and many growth conditions need to be calibrated.

In this EE412 project, we have successfully calibrated the growth recipes for AlGaIn, GaN, and InGaIn on Si (111) substrate. We have also used Hall measurement, I-V measurement, scanning electron microscopy (SEM) and X-ray diffraction (XRD) to characterize the material. After more than 16 rounds and more than 120 hours of successful MOCVD growth, we are glad to announce here that the Axitron-CCS III-N MOCVD tool has been successfully brought up for the epi growth

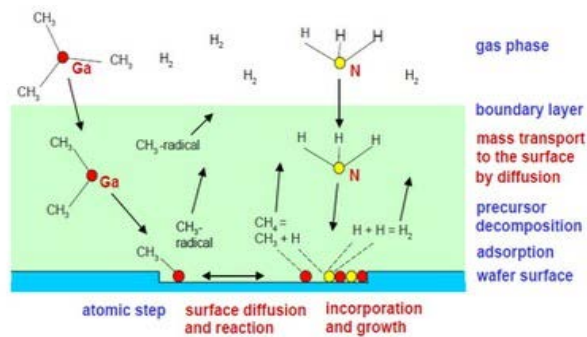
of material for most optoelectronic applications, as well as other applications such as HEMT and multi-junction solar cells.

## II. Methodology and tasks

### a. Introduction to MOCVD growth

MOCVD is the technology behind the multi-billion LED industry, which accommodates for both high crystal quality and high growth rate.

The principle of MOCVD growth can be seen from the figure 2(a). MOCVD utilizes metal organics and hydrides as precursors, and the precursors will react on top of the substrate. Then radicals are absorbed to the substrate surface where the interface reaction. With the deposition of thin-film material, the byproducts are then taken away by the carrier gas flow.



(a)



(b)

Figure 2. (a) Principle of MOCVD. (b) Axitron-CCS system in SNF.

The Aixtron-CCS, as in figure 2(b), is a dedicated high quality III-N system in SNF. It can hold up to one 4-inch wafer, and also has the flexibility of processing coupon-size samples. It has TMIn, TMGa, TMAI and TEGa as growth precursors, Cp2Mg as p-type dopant and SiH4 as n-type dopant. Using those precursors, starting from (111) 4-inch Si substrate, we are able to grow an AlGaN/GaN/InGaN LED, as shown in figure 3. First, a thin layer of AlN needs to be deposited on diffusion-level cleaned Si substrate. Then multi-layer of Al<sub>x</sub>Ga<sub>1-x</sub>N layers need to be grown as buffer layers to adjust the lattice constant. The composition of AlGaN and thickness of each layer need to be calibrated carefully, in order to achieve high material quality and low strain. Finally, a p-i-n heterojunction is deposited as the LED device. Therefore, in order to achieve the high quality LED device on (111) Si substrate, we need to:

- (1) Develop the buffer growth recipe.
- (2) Develop doping recipes for n-type and p-type materials.
- (3) Develop the AlGaN recipe.
- (4) Develop the InGaN recipe.

The buffer layer recipes have been developed by Dr. Xiaoqing Xu. Therefore, in this EE412 project, we mainly focused on (2)-(4).

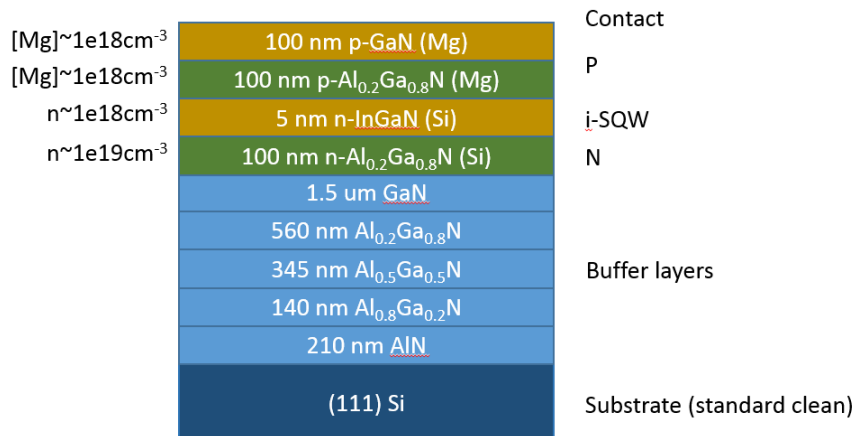


Figure 3. Proposed LED growth

## b. Doping calibration

### i. MOCVD structure

In order to calibrate the doping of GaN and calibrate the composition AlGaN, the following MOCVD recipe was adopted and developed, as in figure 4. On top of the GaN buffer layer, a

thin layer of AlGa<sub>0.2</sub>N is deposited to calibrate the composition and also to insulate the test layer from the buffer layers. Then a layer of doped GaN is grown to calibrate the doping level.

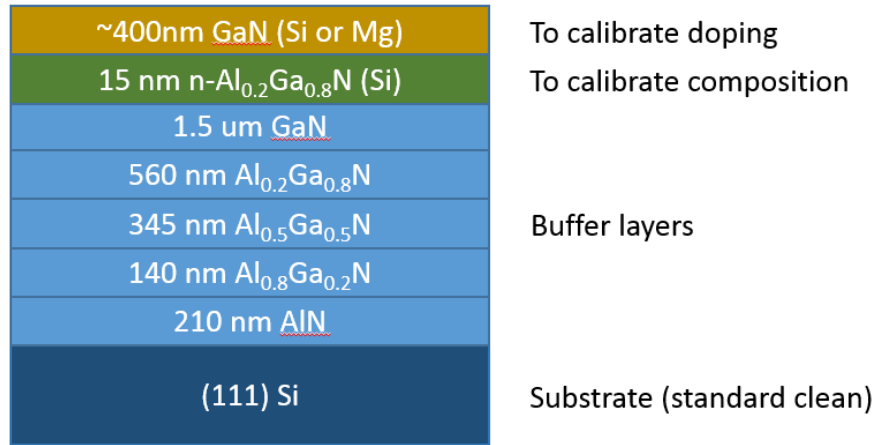


Figure 4. Growth structure for doping calibration

However, the major drawback of this growth structure is that it requires long time (8 hours of growth + 3 hours of baking) to finish the deposition, as there are multi-layer buffer to grow before the actual calibration growth. Therefore, a modified growth strategy is adopted, as in figure 5. First, the buffer layers are grown on a 4-inch Si (111) substrate, which takes around 8 hours. Then the wafer is cut into 6 1/6 4-inch pieces. One important point is that the cut of wafers should be conducted inside the glove box and should use clean tweezers, so as to minimize the potential pollution. Then the top two layers are grown on the 1/6 4-inch piece, which takes around 6.5 hours. In this way, the average growth is reduced to around 7.8 hours per sample.

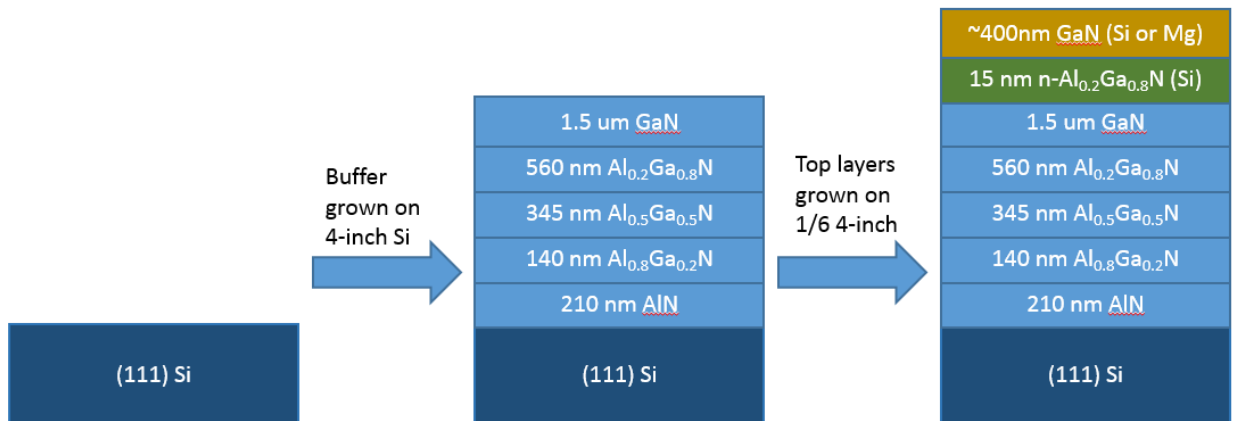


Figure 5. Modified growth strategy.

**ii. Hall measurement**

Hall measurement is one of most important characterization methods to measure the doping density and mobility. In this experiment, we use the H-50 setup in room 152, Paul Allen building, as in figure 6.

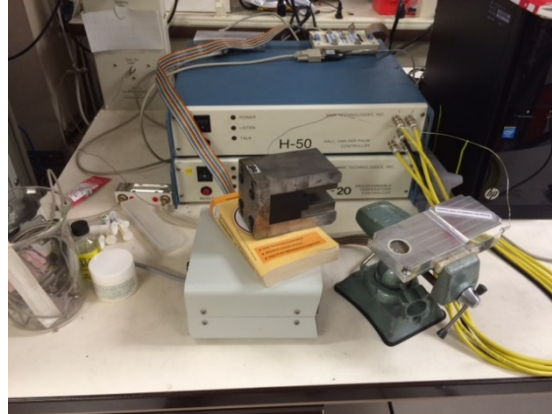
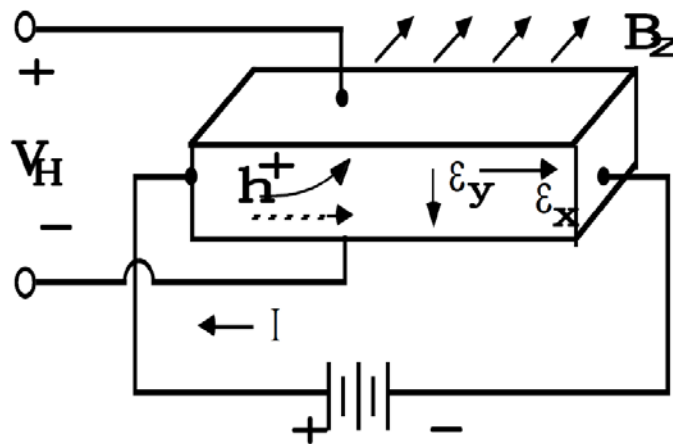


Figure 6. Hall measurement setup

The principle of Hall measurement can be found in [10]. As shown in figure 7(a), voltage is applied at the x direction of a piece of semiconductor, resulting in a current of  $I$ . When the magnetic field is applied at the z direction, due to Lorentz force, the motion of charged carriers will be bended towards different directions at y axis during transportation. Therefore, different types of charge will be accumulated at different sides of the semiconductor, resulting in a built-in electrical field at the y direction. The voltage related to this electrical field is measured as  $V_H$ .



(a)

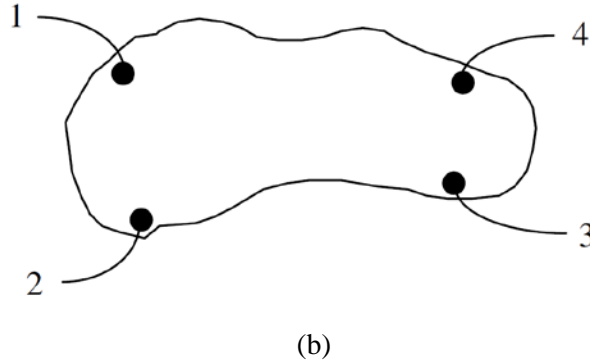


Figure 7. (a) Illustration of Hall measurement [10]. (b) Van Der Pauw method [10].

From hall measurement, we would know Hall coefficient  $R_H$  as

$$R_H = \frac{1}{qp} = \frac{V_H t}{I_x B_z} \quad (\text{II.1})$$

And the doping density  $p$  is  $q \cdot R_H$ .

For mobility:

$$\mu_p = \sigma R_H = \frac{1}{\rho} \frac{V_H t}{I_x B_z} \quad (\text{II.2})$$

The resistivity of this semiconductor can be measured using Van Der Pauw method, as in figure 7(b) [10]. The resistivity is calculated using equation (II.3)

$$\rho = \frac{\pi}{\ln(2)} t \frac{(R_{12,34} + R_{23,41})}{2} F \quad (\text{II.3})$$

### iii. N-GaN

For N-type GaN, we use  $\text{SiH}_4$  as dopant, which has been widely used in the MOCVD industry [11-12]. The major parameter to calibrate is the  $\text{SiH}_4$ -to-Ga molar ratio ( $N_{\text{Si}}:N_{\text{Ga}}$ ). Therefore, we vary the  $\text{SiH}_4$  flow rate so as to achieve different  $N_{\text{Si}}:N_{\text{Ga}}$ , and then we use Hall measurement to measure the mobility, resistivity and doping density. The typical trend of dopant concentration versus  $\text{SiH}_4$  flow rate from a previous research work can be seen in figure 8 [11].

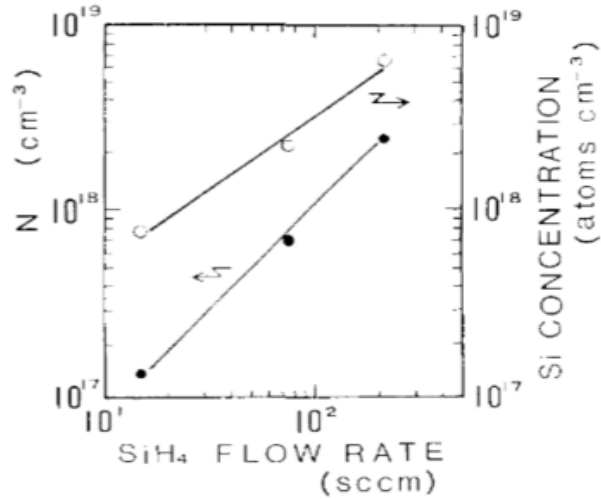


Figure 8. Doping concentration v.s. SiH4 flow rate.

iv. P-GaN

P-GaN was once considered impossible to get, until three Japanese scientists successfully realized it in the 1980s, who also won the Nobel Prize due to this contribution. Akasaki and Amano used the Low-Energy-Electron-Beam-Irradiation (LEEBI) method to activate the p=dopant, while Nakamura utilized high temperature thermal annealing [1]. In this project, we adopt the Nakamura’s method, using Mg as the dopant, which is also the mainstream technology in industry [13-17].

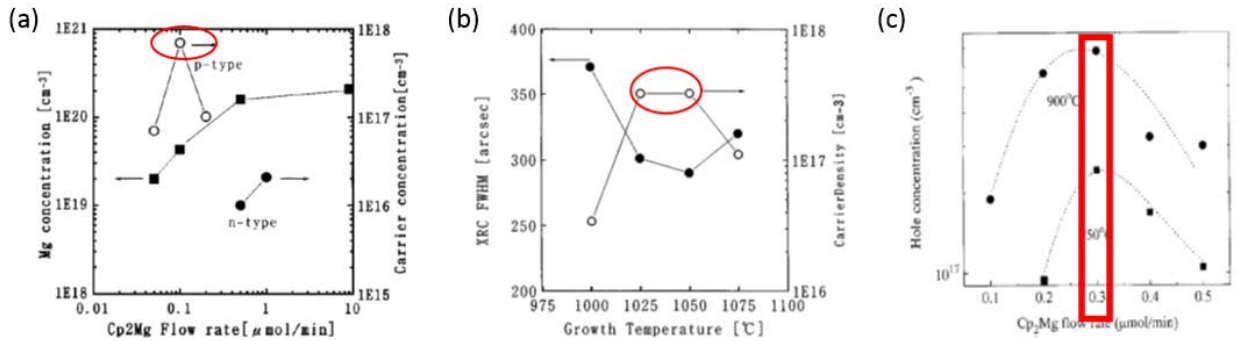


Figure 9. (a) Growth window of  $N_{Mg}:N_{Ga}$ . (b) Growth window of growth temperature. (c) Optimized post-growth anneal condition.



The major challenges of p-GaN growth lie in the three aspects: (1) finding the optimal  $N_{Mg}:N_{Ga}$  ratio, (2) finding the best growth temperature and (3) finding the optimal post-growth annealing condition [13-17]. The difficulty mainly comes from the extremely narrow growth window, as can be seen from figure 9 [13]. For example, the optimal growth temperature window is only 25 C, which is very hard to control.

### c. Ohmic contact for n-GaN and p-GaN

#### i. N-GaN ohmic contact

Ohmic contact is also very important for high quality III-N devices. For n-GaN ohmic contact, Hou et. al. has successfully developed a recipe at SNF, using Ti/Al/Pt/Au metal stack deposited using Innotec [18]. We also adopted this type of contact in our project.

#### ii. P-GaN ohmic contact

Unlike n-GaN contact, ohmic contact for p-GaN has never been developed at SNF. Previous work shows that using Ni/Au double layer with 500C 10-20min annealing in  $N_2/O_2$  ambient should generate ohmic contact for p-GaN [19-21]. In this process Ni is oxidized to  $NiO_x$ , which de-pins the Fermi level at the p-GaN/metal interface. Also, Oxygen would further activate the Mg dopant in GaN, thus further increase the quality of the contact [19-21]. The result of annealing from a previous research work can be seen in figure 10. After annealing, the I-V curve is almost linear, which exhibits good ohmic performance.

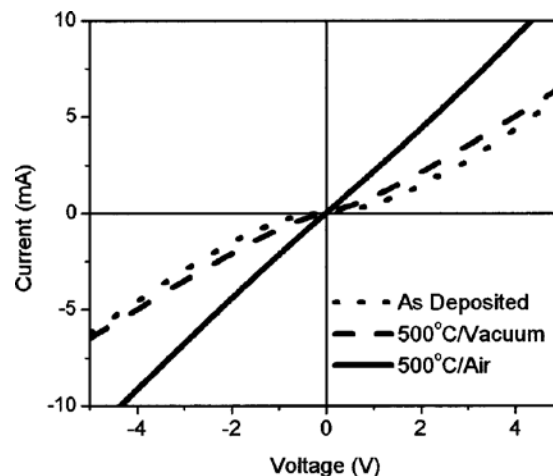


Figure 10. I-V curves of p-GaN contact before and after contact annealing [20].

In this project, we also developed the first ohmic contact recipe for p-GaN at SNF.

#### d. InGaN and AlGaN growth calibration

##### i. InGaN

High-quality InGaN MOCVD layer is essential for high-performance blue LED, as it forms the light-emitting quantum wells due to the lower bandgap of InGaN in the visible light region [22-24]. In this project, we mainly focus on the investigation of the relation between indium composition and the growth temperature. From [22], the In composition should decrease with the increase of growth temperature, as shown in figure 11. We used XRD to verify the indium composition and crystal quality.

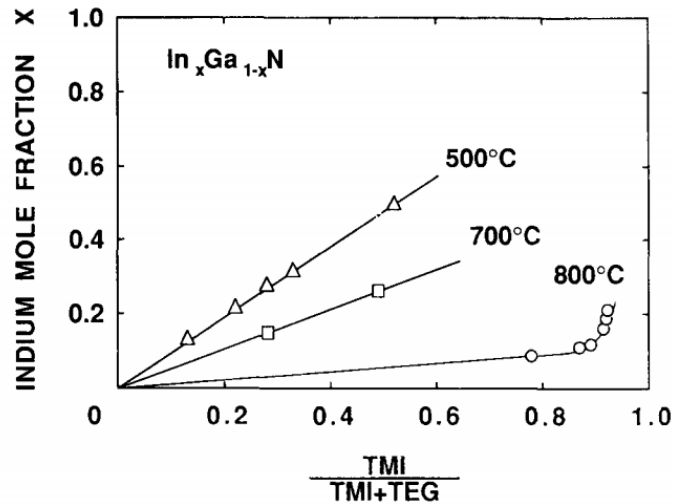


Figure 11. Relation between  $N_{\text{In}}:N_{\text{Ga}}$ , growth temperature and In composition [22].

##### ii. AlGaN

Dr. Xiaoqing Xu has already successfully developed recipe for AlGaN growth. In this project, we verified the growth thickness of  $\text{Al}_{0.2}\text{Ga}_{0.8}\text{N}$ , which may act as the barrier layer for future hetero-junction III-N LED device.

#### e. Summary of project tasks

##### i. N-GaN

- Investigate relation between doping density and SiH<sub>4</sub> flow rate, or Si-to-Ga ratio.

**ii. P-GaN**

Investigate relation between doping density and

- Mg flow rate, or Mg-to-Ga ratio.
- Growth temperature.
- Annealing temperature.

**iii. InGaN**

- Investigate relation between indium composition and growth temperature
- Verify crystal quality

**iv. AlGaN**

- Verify growth thickness for Al<sub>0.2</sub>Ga<sub>0.8</sub>N.

### **III. Experiment Results**

**v. n-GaN**

As elaborated in the previous section, we focused on experimentally extracting the relation between the molar ratio ( $N_{Si}:N_{Ga}$ ) and the electron density in n-GaN.

We first grew the test structure as shown in the previous section with different SiH<sub>4</sub> flow rates. All other growth parameters, including the growth temperature, pressure and TMGa flow rate are kept constant. Next, we cut the grown samples into pieces with proper size and use electron-beam evaporation to coat a Ti (20 nm) / Al (100nm) / Pt (80 nm) contact, followed by a 35 sec rapid thermal annealing (RTA) in N<sub>2</sub> at 850C. The samples are then characterized using scanning electron microscope (SEM), I-V probe station and the H-50 Hall measurement setup.

Figure 12(a) shows a typical SEM image of the cross-section view of a grown sample. It is shown that the interfaces of the epi-layers are smooth, and the target thickness of n-GaN has been reached. 370 nm is the typical thickness of the n-GaN samples.

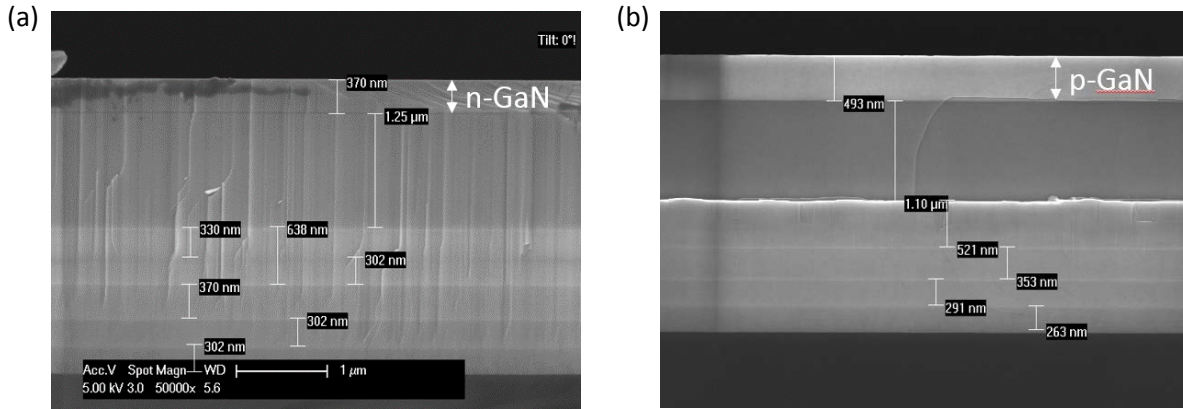


Figure 12. SEM cross-section image of a MOCVD grown (a) n-GaN (b) p-GaN sample.

To ensure good contact quality, we measured the I-V characteristics of the n-GaN film. Each of the two diagonal contact pairs was probed. Figure 13 shows the I-V curves of a typical sample before and after RTA. It is shown that the thin film has good conductivity and contacts are perfectly ohmic. It is also shown that the RTA process does not significantly affect the contact quality.

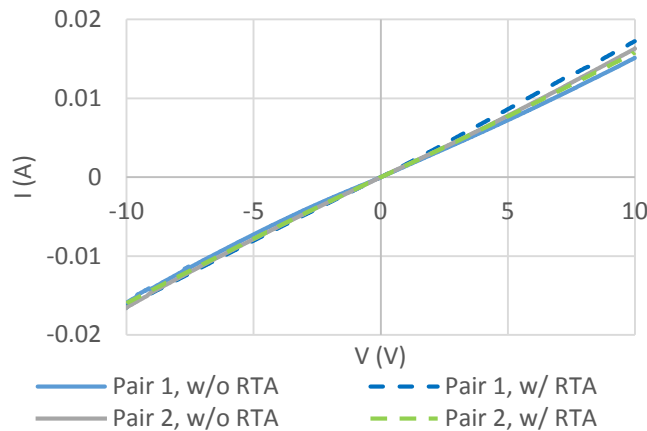


Figure 13. I-V curves of an n-GaN sample measured with probes on each of the diagonal contact pairs. Solid lines are result before RTA and dash lines after RTA.

We conducted multiple rounds of growth, in which three rounds led to significant experiment results. Table 1 shows the growth parameters and the Hall measurement result. Figure 14 shows

the plots of the mobility, resistivity and carrier density versus  $N_{Si}:N_{Ga}$ . The listed growth temperature in table 1 is the temperature set in the recipe, not the actual temperature on the growth surface during the process, which is approximately 90C-150C lower than the set growth temperature. Detailed information regarding the relation between set growth temperature and actual growth temperature can be found in [9].

Ga Flow (sccm)	40.5	6.75	40.5
SiH4 Source/ Dilute/ Push (sccm)	9/981/7	9/981/35	10/100/7
$N_{Si}:N_{Ga}$	2.53E-06	1.27E-05	2.53E-05
Growth Temp (C)	1295	1295	1295
Growth Time (sec)	680	680	680
Growth Pressure (mbar)	200	200	200
Thickness (nm)	352	352	352
Mobility (cm <sup>2</sup> /Vs)	3.2E+02	1.7E+02	1.9E+02
Resistivity (ohm*cm)	0.45	0.016	0.013
Electron Density (cm <sup>-3</sup> )	4.4E+16	2.3E+18	2.4E+18

Table 1. Growth parameters and Hall measurement results for n-GaN

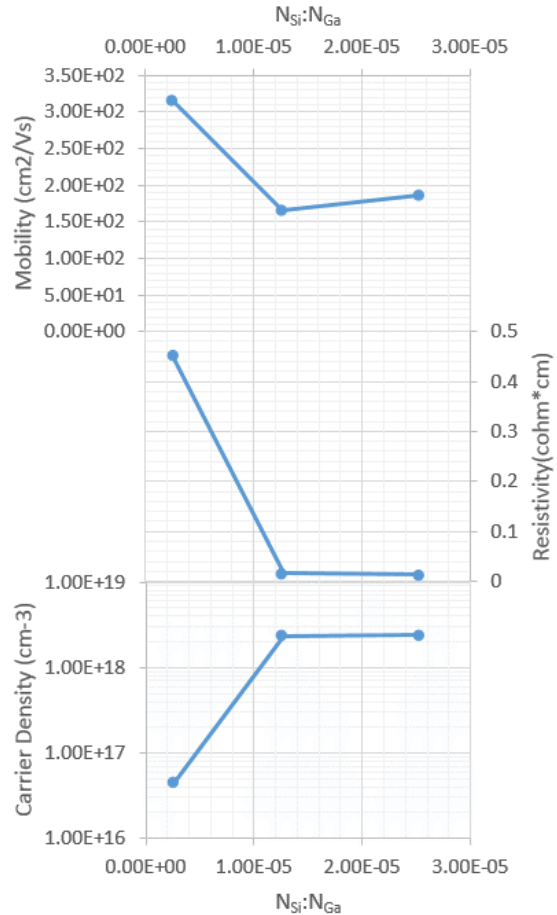


Figure 14. Plots of mobility, resistivity and carrier density versus  $N_{Si}:N_{Ga}$ .

We can see that an electron density of  $> 2 \times 10^{18} \text{ cm}^{-3}$  has been achieved, which is sufficient for most optoelectronic applications. The mobility and resistivity values also indicate good material quality. It also suggests that the carrier density can be well controlled in the  $4 \times 10^{16} \sim 2 \times 10^{18} \text{ cm}^{-3}$  range. The trend can be further investigated with additional growths setting  $N_{Si}:N_{Ga}$  to be in the range of  $2 \times 10^{-6} \sim 2 \times 10^{-5}$ .

vi. p-GaN

For the p-GaN doping calibration, we used Mg as the dopant atom and Bis(cyclopentadienyl)magnesium (Cp2Mg) as the doping material. We followed the same experiment procedure as described above for the n-GaN except for a few changes: after the MOCVD growth, the samples stayed in the growth chamber for a 20 ~ 30 min post-growth annealing to activate the dopant. The metal recipe used to make the contact is Ni (20 nm)/Au(20 nm), with a 10 min, 500C RTA in a O<sub>2</sub>(20%) /N<sub>2</sub>(80%) atmosphere. We also tried 10-30min baking at 500C-550C in air using a hot-plate. However, the performance of contact was degraded after such baking, which may be due to the water vapor in the atmosphere.

As described in the previous section, p-GaN doping condition is very complicated. There are three main control variables: the molar ratio  $N_{Mg}:N_{Ga}$ , the growth temperature and the annealing temperature. Other condition parameters, such as the annealing time, may also have some effects on the result, but are assumed only secondary in our experiments.

Figure 15 shows the experiment parameter matrix and the search path for the ideal growth window. As shown in the previous work, p-GaN has a very narrow growth window. Due to the limit of time and material we were not able to exhaust the matrix, instead we relied on the trend observed in the previous experiments to determine the condition for the next experiment.

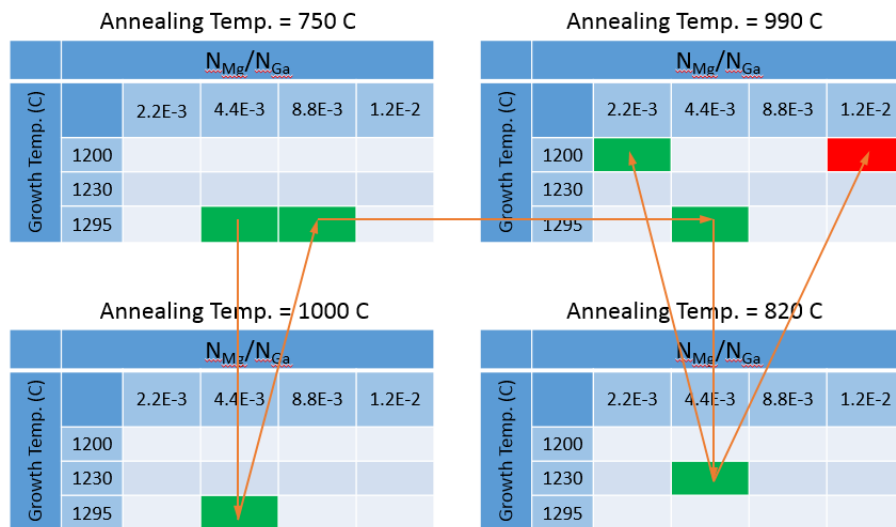


Figure 15. Parameter matrix for the p-GaN doping calibration and the growth window search path (orange arrows). Green blocks indicate experiments that had been conducted and the red block indicates the search destination with the optimal growth condition.

Figure 12(b) shows the SEM image of a typical p-GaN sample, which shows the same quality as the n-GaN. Figure 16 shows the I-V curves of p-GaN samples with/without RTA and with different carrier density. The thin film appears to have lower conductivity than n-GaN and the contact is not always ohmic. It shows that the contact will be ohmic only if the carrier density is sufficiently high, which makes the calibration of low doping very challenging. In addition, as it is observed, RTA appears to improve the contact quality, though further experiment needs to be conducted to find the optimal RTA recipe.

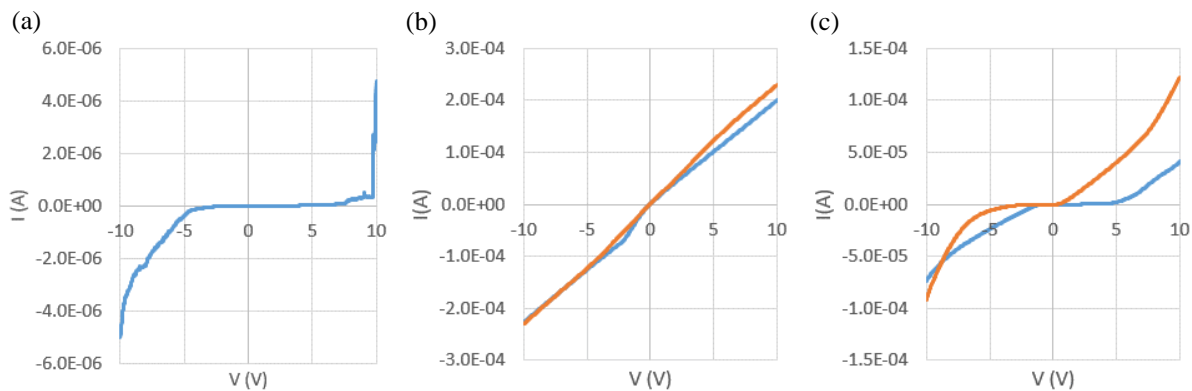


Figure 16. I-V curves of p-GaN sample measured with probes on each of the diagonal contact pairs (denoted by different colors). The samples have different doping and contact annealing conditions: (a) contact not annealed (b) 500C RTA, doping high enough for an ohmic contact (c) 500C RTA, doping not high enough for an ohmic contact.

Table 2 shows the growth parameters and the Hall measurement result. As the contact for low-doping samples did not have good quality, some of the data in the table were reasonable estimation based on limited measurement accuracy. Figure 17 shows the observed trends of the variation of mobility, resistivity and carrier density to the molar ratio, growth temperature and annealing temperature. More experiments need to be conducted in order to make the results more accurate.

Ga Flow (sccm)	13.5	13.5	6.75	13.5	13.5	5	13.5
Mg Flow (sccm)	200	200	200	200	200	200	100
$N_{Mg}:N_{Ga}$	4.4E-31	4.4E-3	8.8E-3	8.8E-3	4.4E-3	1.2E-2	2.2E-3
Growth Temp. (C)	1295	1295	1295	1230	1230	1200	1200
Growth Time (sec)	2040	2040	4080	2040	2040	2040	2040

Growth Pressure (mbar)	200	200	200	200	200	400	200
Annealing Temp (C)	750	1000	750	990	820	990	990
Annealing Time (sec)	1200	1200	1200	1800	1800	1800	1800
Annealing Pressure (mbar)	950	950	950	950	950	950	950
Thickness (nm)	425	350	336	450	500	200	500
Mobility (cm <sup>2</sup> /Vs)	10	4.3	7.6	20	4.5	5.3	97
Resistivity (ohm * cm)	1.3E+02	1.5E+03	1.7E+03	4.0E+01	2.3E+02	1.0E+00	1.1E+01
Hole Density (cm <sup>-3</sup> )	9.4E+14	1.0E+16	4.8E+14	7.8E+15	6.0E+15	1.3E+18	5.3E+19

Table 2. Growth parameters and Hall measurement results for p-GaN. Red font indicates data of reasonable estimation based on limited measurement accuracy

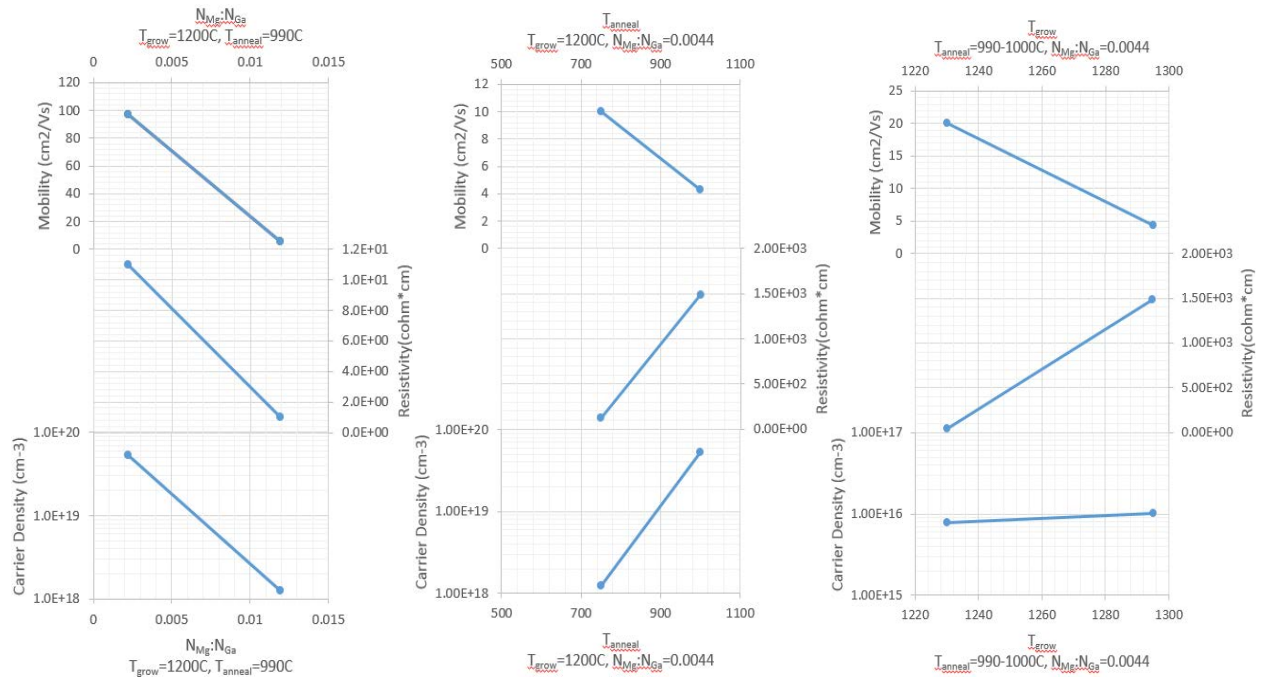


Figure 17. Plots of mobility, resistivity and carrier density versus  $N_{Mg}:N_{Ga}$ , growth temperature and annealing temperature. The controlled variables are listed in the x-axis labels.

In spite of the great challenges in conducting the calibration, we successfully found a growth window which allows us to growth p-GaN with a hole density  $> 1 \times 10^{18} \text{ cm}^{-3}$ , which is sufficient for most optoelectronic applications. More investigation on the growth window needs to be done in order to accurately control the doping of p-GaN.

## vii. InGaN



We conducted two rounds of InGaN growth to verify the crystal quality and indium/gallium composition. We grew the samples using the parameters specified in Table 3 and then used SEM and X-ray diffraction (XRD) to characterize the samples. No metal contact is needed. The indium/gallium composition depends on mainly the growth temperature, so we varied the growth temperature and investigated the relation between the growth temperature and the indium percentage in the alloy.

Ga Flow (sccm)	41	41
In Flow (sccm)	202	202
$N_{In}:N_{Ga}$	1.42	1.42
NH3 Flow (sccm)	4000	4000
Growth Temp (C)	790	850
Growth Time (sec)	2700	2700
Growth Pressure (mbar)	400	400
Thickness (nm)	250	170

Table 3. Growth parameters for InGaN.

Figure 18 shows the SEM images of the two InGaN samples with different growth temperature. Figure 19 shows the XRD spectra of the two InGaN samples. From the XRD results we extracted the InGaN(0002) peak position at 32.84 degree for the 850C sample and 32.54 degree for the 790C sample, which indicates a indium percentage of ~36% for the former and ~45% for the latter. On the XRD spectrum it can also be seen that the main peak in both (0002) and (0004) directions were intact, indicating no phase separation. Therefore, we successfully achieved high-quality growth of InGaN with indium composition as high as 45%, which is remarkable comparing to the results from previous research work [22-24]. Nevertheless, further calibration is needed for accurate control of InGaN growth.

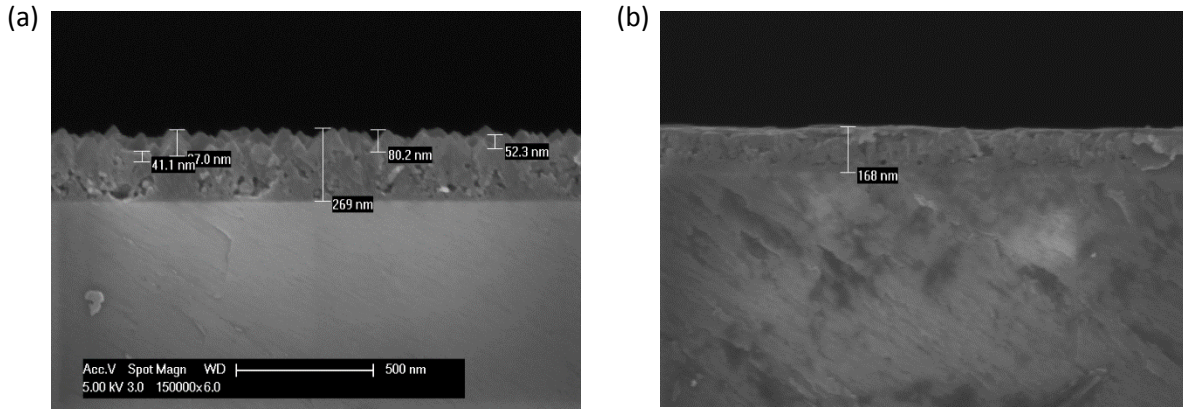


Figure 18. SEM cross-section image of MOCVD grown InGaN under growth temperatures of (a) 850C (b) 790C.

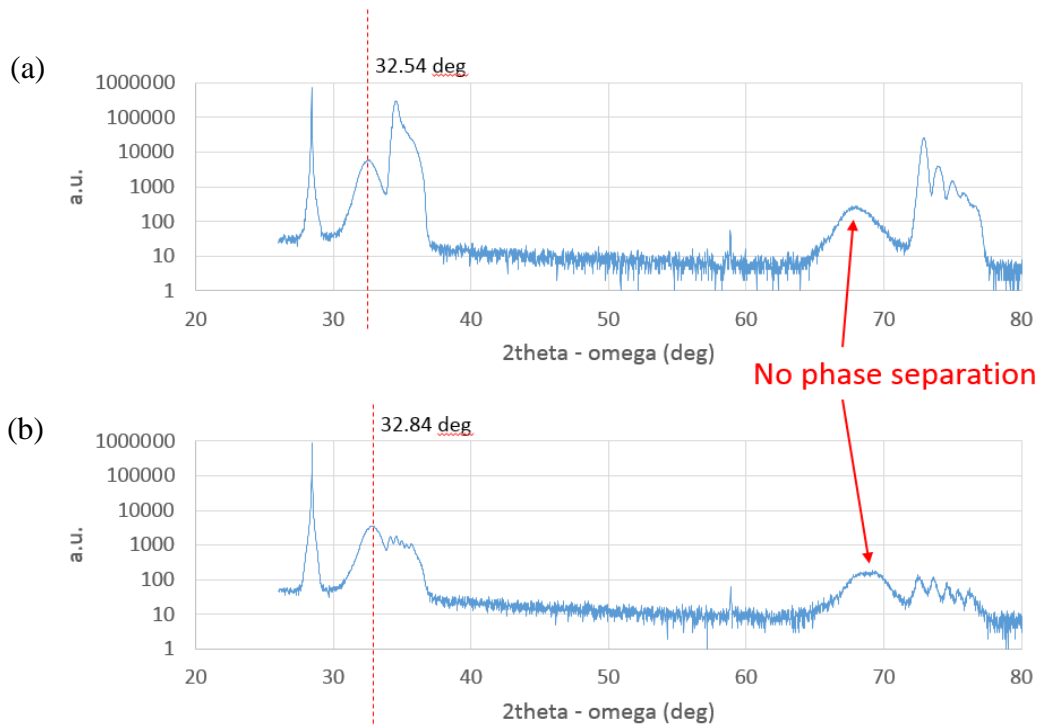


Figure 18. XRD spectrum of MOCVD grown InGaN under growth temperatures of (a) 850C (b) 790C. InGaN peak location are marked.

viii. AlGaN

Although AlGa<sub>N</sub> growth calibration is not the focus of this work, we also verified the thickness of AlGa<sub>N</sub> growth using certain recipe, as specified in Table 4. The growth condition corresponds to a composition of approximately 20% Al and 80% Ga, from previous calibration result.

Al Flow (sccm)	Ga Flow (sccm)	N <sub>Al</sub> :N <sub>Ga</sub>	NH <sub>3</sub> Flow (sccm)	Growth Temp (C)	Growth Time (sec)	Growth Pressure (mbar)	Thickness (nm)
5.5	7.6	0.1043	6.70E+02	1295	180	100	23

Table 4. Growth parameters for AlGa<sub>N</sub>.

Figure 19 show SEM image of the cross-section view of the AlGa<sub>N</sub> layer, which is measured to have a thickness of ~23 nm, indicating a growth rate of ~1.2 Å/s.

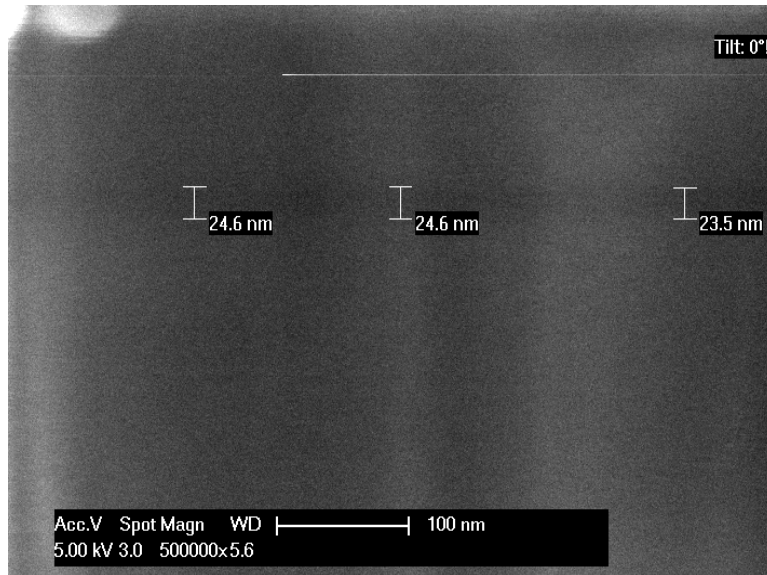


Figure 19. SEM cross-section image of a MOCVD grown AlGa<sub>N</sub> sample, sandwiched between two Ga<sub>N</sub> layers.

#### ix. Other Contribution

From this work we also gained a few insight on the growth using the Aix-ccs MOCVD tool and subsequent processes:

a) The tool always needs an 1100C baking step after each growth to maintain good chamber condition. For a growth time of ~40 min, 90 min of baking has shown to be sufficient. However, 60 min of baking has shown to be slightly insufficient, mild residue was still observed.

**b)** Indium can also be used to make ohmic contact for n-GaN, but was observed to have inferior quality than Ti/Al/Pt.

**c)** For p-GaN contact, RTA annealing has shown to be effective in improving the contact quality. The RTA recipe has been specified in the previous section. The optimal RTA recipe may need further calibration.

#### **IV. Summary and future work**

In summary, we have successfully calibrated multiple important recipes on the new III-N Aixtron-CCS MOCVD system for SNF. For the first time, we have achieved n-GaN and p-GaN with controllable doping level. In addition, we have also successfully grown AlGaIn and InGaIn on (111) Si substrate with good crystal quality.

We also would like to propose some future work for people who are interested in taking EE412 with this III-N MOCVD tool. Those work may include:

- Calibrate lower doping of p-GaN.
- More InGaIn and AlGaIn calibration.
- LED growth and fabrication.

#### **V. Acknowledgement**

- Thanks to Xiaoqing for the mentorship, training on the MOCVD system and other help on the project.
- Thanks to Prof. Howe, Dr. Mary Tang and other EE412 mentors for their valuable advice.
- Thanks to Prof. Harris for providing funding for SEM and other characterization tools.

## References

- [1] [http://www.nobelprize.org/nobel\\_prizes/physics/laureates/2014/](http://www.nobelprize.org/nobel_prizes/physics/laureates/2014/)
- [2] <http://www.navigantresearch.com/newsroom/led-lighting-will-constitute-nearly-94-percent-of-annual-street-lighting-sales-worldwide-by-2023>
- [3] <http://proj.ncku.edu.tw/research/articles/e/20081219/1.html>
- [4] EE216 Lecture notes
- [5] Dadgar, A., et al. "Thick, crack-free blue light-emitting diodes on Si (111) using low-temperature AlN interlayers and in situSixNy masking." *Applied physics letters* 80.20 (2002): 3670
- [6] Lahreche, H., et al. "Optimisation of AlN and GaN growth by metalorganic vapour-phase epitaxy (MOVPE) on Si (111)." *Journal of crystal growth* 217.1 (2000): 13-25.
- [7] Ishikawa, Hiroyasu, et al. "GaN on Si substrate with AlGa<sub>N</sub>/AlN intermediate layer." *Japanese journal of applied physics* 38.5A (1999): L492.
- [8] Krost, Alois, and Armin Dadgar. "GaN-based optoelectronics on silicon substrates." *Materials Science and Engineering: B* 93.1 (2002): 77-84.
- [9] <https://snf.stanford.edu/SNF/equipment/chemical-vapor-deposition/mocvd/aix-ccs>
- [10] Schroder, Dieter K. *Semiconductor material and device characterization*. John Wiley & Sons, 2006.
- [11] Koide, N., et al. "Doping of GaN with Si and properties of blue m/i/n/n+ GaN LED with Si-doped n+-layer by MOVPE." *Journal of crystal growth* 115.1 (1991): 639-642.
- [12] Rowland, L. B., K. Doverspike, and D. K. Gaskill. "Silicon doping of GaN using disilane." *Applied physics letters* 66.12 (1995): 1495-1497.
- [13] Tokunaga, H., et al. "Growth condition dependence of Mg-doped GaN film grown by horizontal atmospheric MOCVD system with three layered laminar flow gas injection." *Journal of crystal growth* 189 (1998): 519-522.
- [14] Kozodoy, Peter, et al. "Heavy doping effects in Mg-doped GaN." *Journal of Applied Physics* 87.4 (2000): 1832-1835.
- [15] Götz, W., et al. "Activation of acceptors in Mg - doped GaN grown by metalorganic chemical vapor deposition." *Applied Physics Letters* 68.5 (1996): 667-669.
- [16] Sheu, Jinn-Kong, and G. C. Chi. "The doping process and dopant characteristics of GaN." *Journal of Physics: Condensed Matter* 14.22 (2002): R657.
- [17] Huang, Jen-Wu, et al. "Electrical characterization of Mg - doped GaN grown by metalorganic vapor phase epitaxy." *Applied physics letters* 68.17 (1996): 2392-2394.

- [18] Hou, Minmin, and Debbie G. Senesky. "Operation of ohmic Ti/Al/Pt/Au multilayer contacts to GaN at 600° C in air." *Applied Physics Letters* 105.8 (2014): 081905.
- [19] Qiao, D., et al. "A study of the Au/Ni ohmic contact on p-GaN." *Journal of Applied Physics* 88.7 (2000): 4196-4200.
- [20] Sheu, J. K., et al. "High-transparency Ni/Au ohmic contact to p-type GaN." *Applied physics letters* 74.16 (1999): 2340-2342.
- [21] Ho, Jin-Kuo, et al. "Low-resistance ohmic contacts to p-type GaN." *Applied physics letters* 74.9 (1999): 1275-1277.
- [22] Matsuoka, T., et al. "Wide-gap semiconductor InGaN and InGaAlN grown by MOVPE." *Journal of electronic materials* 21.2 (1992): 157-163.
- [23] Egawa, T., B. Zhang, and H. Ishikawa. "High performance of InGaN LEDs on (111) silicon substrates grown by MOCVD." *Electron Device Letters, IEEE* 26.3 (2005): 169-171.
- [24] Sheu, Jinn-Kung, et al. "Low-operation voltage of InGaN-GaN light-emitting diodes with Si-doped In/sub 0.3/Ga/sub 0.7/N/GaN short-period superlattice tunneling contact layer." *Electron Device Letters, IEEE* 22.10 (2001): 460-462.